ELSEVIER

Journal of Chromatography A, 948 (2002) 203–223

JOURNAL OF CHROMATOGRAPHY A

www.elsevier.com/locate/chroma

# Streaming potential in open and packed fused-silica capillaries

Isabelle Gusev, Csaba Horváth*

*Department of Chemical Engineering, Yale University, P.O. Box 208286, New Haven, CT 06520-8286, USA*

**Abstract**

The surface properties of novel stationary phases in packed and open tubular columns for capillary electrochromatography (CEC) were examined by measuring the streaming potential in a home made apparatus. The surfaces investigated include materials such as porous styrenic sorbents and octadecyl-silica as well as fused-silica tubing, in both raw and surface modified forms. Functionalization of the surface was carried out, for instance, by reductive amination or organosilane grafting on to capillary inner wall. The dependence of the streaming potential on pH was examined with aqueous solutions in the pH range from 2.5 to 9.0. Electrokinetic properties of 50 μm I.D. fused-silica capillaries have been determined by both streaming potential and electrosmotic flow measurements. Both methods gave similar pH profiles of the $\zeta$-potential and the isoelectric points. This confirms the viability of our approach to evaluate the specific charged groups of the packing which is one of the important factors influencing electrosmotic flow (EOF) velocity and protein adsorption during a chromatographic run. In addition to bare silica capillaries, styrenic monolithic columns with different surface functionalities, which have been extensively used in our laboratory for CEC separation of peptides and proteins, were employed for comparison of two methods. Plots of zeta potential as a function of percent ACN show a complex behavior, indicating that zeta potential cannot be predicted simply from binary mixture solvent properties. It is demonstrated that the evaluation of the zeta potential by the streaming potential method is nondestructive, relatively fast, without untoward effects introduced by Joule heating and yet another means for the characterization of the surfaces under conditions employed in CEC. 

*Keywords:* Streaming potential; Zeta potential; Packed columns; Surface characterization

## 1. Introduction

In capillary electrochromatography (CEC) the mobile phase is electrosmotically driven across the column at a rate determined by the properties of both the stationary and the mobile phases. So far, in most applications of CEC the stationary phases and operating conditions have been similar to those commonly used in reversed-phase chromatography [1–8]. Thus, the main attention has been focused on the enhancement of the column efficiency [6,8]. Recent development of novel stationary phases and the employment of appropriate operating conditions show that the combination of chromatographic retention and electrophoretic migration can impart unique selectivity to the separation process by CEC [9–15]. Strategies for the development of new materials with improved retention mechanism have to be based on comprehensive studies of interfacial properties.

Novel porous monolithic packings have been prepared and appropriately functionalized to obtain the desired chromatographic surfaces. They are specially tailored to exploit the full potential of CEC

*Corresponding author. Tel.: +1-203-432-4357; fax: +1-203-432-4360.

*E-mail address:* csaba.horvath@yale.edu (Cs. Horváth).

0021-9673/02/$ – see front matter 
PII: S0021-9673(01)01450-9

arising from the combined separation powers of chromatographic retention and electric field for the separation of peptides and proteins [16–18]. In most cases porous monolithic support was functionalized in situ in order to attach ionogenic functions and chromatographic binding sites to the surface, thus producing an *amphiphilic* [19] stationary phase.

During the course of research in our laboratory it has become evident that the design and synthesis of new capillary packing materials for CEC can benefit from the knowledge of their electrokinetic characteristics. In order to evaluate electrokinetic properties of the packing potentially interesting for electrochromatography, an experimental set-up for streaming potential measurements in packed and open tube fused-silica capillaries was built in this work. The study is carried out at different pH values, ionic strengths and electrolytes with capillaries of 50 and 75 μm I.D. The results are expected to demonstrate the feasibility of streaming potential method, and perhaps, to give insight into the complex aspects of surface phenomena in CEC.

## 2. Zeta potential and its measurements

Electrokinetic properties of surfaces are most frequently characterized in terms of the pH profile of their zeta potential ($\zeta$), which is the potential at the plane of shear [20]. The exact location of the shear plane is debatable, but it is reasonable to place it at the inner plane of the diffuse layer. The arrangement of charges on the stationary phase surface and the charges in the liquid phase is referred to as the *electrical double layer* at the interface.

Since first observed in 1807 [21], electrokinetic phenomena, i.e. electrosmosis and electrophoresis, have been studied intensively. In 1859, it was first proposed [22] that the converse of the phenomena producing electrosmosis would give rise to electrical current and could be used to generate electricity. Depending on whether the electric current occurs as the cause or as the result and whether the liquid or the solid body is at rest, electrokinetic phenomena are divided into four categories as shown in Fig. 1. von Smoluchowski designated this entire class of phenomena with the common name, electroendosmotic or, in short, electrosmotic phenomena [23]. All these phenomena are due to the existence of the electrical double layer, i.e. the separation of charge that occurs at the interface between two phases.

According to the Gouy–Chapman–Stern–Grahame model, the space charge in the electrolyte solution is divided into two regions: the immobile (Stern) region very near the wall with a sharp fall of potential within the Stern layer, from $\psi_o$ (surface potential) to $\psi_s$ (Stern potential) and a diffuse region, where the distribution of electrical potential is usually described by the Poisson–Boltzmann equation [20]:

$$\nabla^2\psi = \frac{d^2\psi}{dx^2} = -\frac{1}{\varepsilon}\sum_i n_i^o z_i e \exp\left(\frac{-z_i e\psi}{kT}\right) \quad (1)$$

where $\psi$ is the local (average) value of the electrical potential; $e$ is the elementary charge; $\varepsilon = \varepsilon_r\varepsilon_0$ is the absolute permittivity [24], i.e. $\varepsilon_0$ is the permittivity of vacuum, $\varepsilon_r$ is the dielectric constant of the mobile phase; and $z_i$ and $n_i^o$ are the number of charges and the bulk number concentration, respectively, of ion $i$. This is a nonlinear differential equation which has been solved analytically for a flat interface and for a symmetric $z$:$z$ electrolyte to yield:

$$\frac{\exp\left(\frac{ze\psi_x}{2kT}\right)-1}{\exp\left(\frac{ze\psi_x}{2kT}\right)+1} = \frac{\exp\left(\frac{ze\psi_s}{2kT}\right)-1}{\exp\left(\frac{ze\psi_s}{2kT}\right)+1}\exp(-x\kappa) \quad (2)$$

where $\kappa$ is the Debye–Hückel screening factor and is directly proportional to the square root of the electrolyte concentration. This is the Gouy–Chapman expression for the variation of potential within the double layer without the simplifying assumption of low potentials. The numerical value of the $\zeta$-potential is directly dependent on the location of the shear plane within the electrical double-layer, which is itself related to flow conditions at the solid–liquid interface and is unknown. It is generally agreed that this surface of shear occurs within the diffuse part of the electrical double layer, near to the Outer Helmholtz Plane [20].

Zeta potentials may be evaluated from experimental data on any of the four electrokinetic effects: streaming potential, electrosmotic flow velocity, sedimentation potential, and electrophoresis — pro-

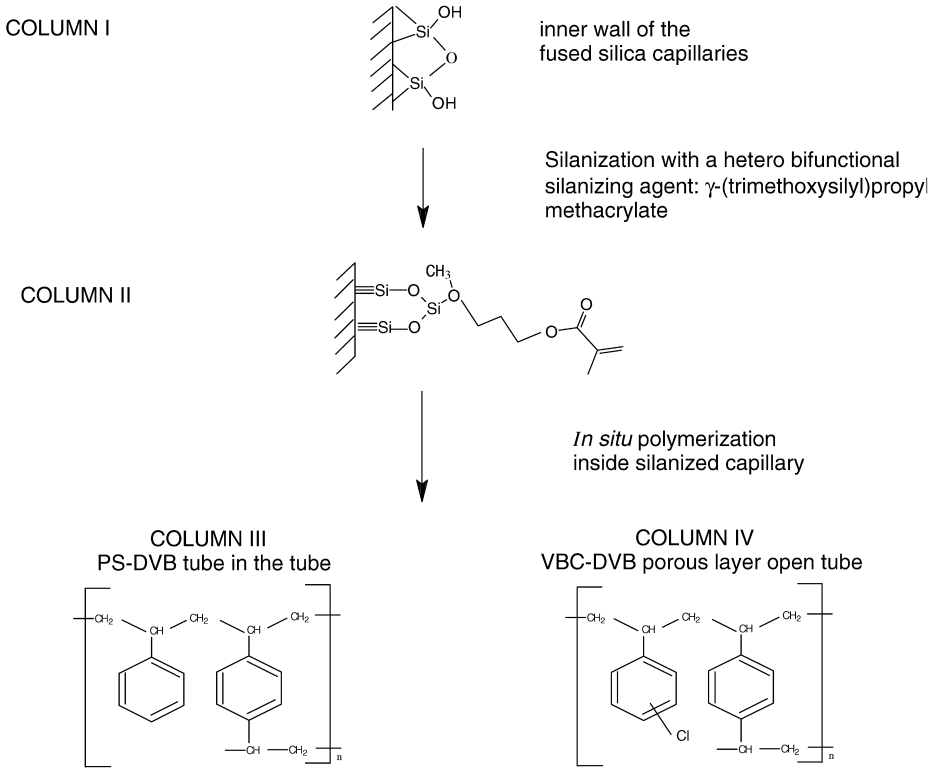


Fig. 1. Preparation of monolithic support.

vided certain other properties of the system under consideration are known. The most widely used procedure, electrophoresis, is effective in dilute systems where electrokinetic properties of the individual particles are commonly studied, thus the imposed field is in interaction with isolated particles only and, hence, theory is relatively simple.

Electrokinetic investigations on porous plugs, however, are much more elaborate than electrophoresis but it has the advantage that $\zeta$-potentials of large particles and porous monoliths can be determined. Although electrophoresis can be used to determine the zeta potential of a monolithic sample after grinding, the newly formed surface can differ considerably [25] from the stationary phase surface, as in the case of coatings or surface modifications. Moreover, hydrophobic polymer packings that are usually not assessable in dispersed form in neat aqueous solutions by electrophoresis can be analyzed by streaming potential or electrosmotic measurements in aqueous buffers used in CEC. It may finally be noted that, because in CEC packings the area/liquid volume ratio is not small, the danger of contamination is much less than in microelectrophoresis.

Theoretically, the zeta potential calculated for identical surfaces should be independent of the particular electrokinetic phenomena under investigation. A number of comparisons relating to essentially flat surfaces have been made and in general moderate correlation has been found [26], for example, between electrophoretic and electrosmotic data for octadecanol [27] and between electrosmotic flow and streaming potential data for softwood, cotton, cellulose acetate and glass fibers [28]. During the last several years, substantial interest has arisen from the observation of an apparent discrepancy between the results obtained by different electrokinetic methods for a given system [29,30]. Theoretical interpretation of the measured electrokinetic quantities is always based on a number of explicit and implicit assumptions. Since the meaning of the obtained data de-

pends on the adequacy of the theory used for their interpretation, the underlying assumptions are often questioned and discussed in the literature. Less so with the smooth surfaces, however, the case of the rough or hairy solid surface is much more complicated, because the surface roughness affects not only the position of the shear plane but also the surface charge density distribution and the surface conductivity. Hence, the interpretation of data for these more complex systems requires the application of two or more electrokinetic techniques in order to obtain complimentary information.

The main difficulty in comparing $\zeta$-potentials from electrophoresis to those from electrosmosis or streaming potential is that of ensuring identical surfaces; this difficulty does not arise when comparing electrosmosis with streaming potential, since the same column can be used for both determinations.

Streaming potential is generated upon forcing an electrolyte solution through porous monolithic or granular column packing. The charges present in the mobile part of the double layer are carried towards the column end and their accumulation sets up an electric field. The resulting electrical potential difference between the two sides of the porous packing, i.e. between the inlet and outlet of the packed capillary column, is called the streaming potential [20].

If the flow is slow enough to be streamlined, i.e. the Poiseuille's law is applicable, the streaming potential is related to the $\zeta$-potential by the modified [31] Helmholtz–von Smoluchowski equation:

$$U_{sp} = \frac{\varepsilon_r \varepsilon_o \zeta P}{\eta \lambda} F_1(\kappa r, \psi_o) \quad (3)$$

where $\eta$ is the viscosity, $\lambda$ is the conductivity of the liquid in the capillary column, $U_{sp}$ is the streaming potential resulting when the liquid is forced through the capillary under the pressure $P$, and $F_1(\kappa r, \psi_o)$ is the correction factor which depends on the magnitude of the electrokinetic radius and the surface potential [31].

In contrast, electrosmotic flow (EOF) in packed and open capillaries originates from an electric double layer when an electric field is applied over the length of the capillary. The migration velocity of a neutral marker molecule can be used to estimate the EOF [32]. The magnitude of the EOF depends on the applied electric field, $E$, and on the distribution of charges in the interfacial layer according to the modified Helmholtz–von Smoluchowski equation for the electrosmotic flow velocity, $u_{eo}$, of an electrolyte solution along a flat charged surface under the influence of the electric field:

$$u_{eo} = \frac{\varepsilon_r \varepsilon_o \zeta E}{\eta} F_1(\kappa r, \psi_o) \quad (4)$$

Both Eqs. (3) and (4) are applied to a vessel of nonconducting material of random shape and are based on the following assumptions [23]:

(1) The viscosity at the surface is the same as that of the bulk fluid;

(2) The liquid motion is a ''slow'' flow, which means that in the hydrodynamic equations the terms originating from the kinetic energy are to be disregarded when compared to the effect of viscosity;

(3) The external potential gradient is simply superimposed on the potential gradient of the double layer.

For a plug of an arbitrary geometry, von Smoluchowski [33] has shown that Eqs. (3) and (4) with correction factor equal to unity remain valid provided the pore diameter is much larger than the double layer thickness. This is an advantage of measuring streaming potentials over streaming currents that in the limiting case, the measured signal is independent of the packing geometry.

Understanding, predicting and controlling the EOF in CEC demands a measuring technique that closely resembles the experimental separation conditions. Among the methods for the determination of $\zeta$-potential, streaming potential gives the most precise measurements, since all of the quantities involved in the computation are measurable with greater accuracy and less difficulty than those in the other methods [34].

Streaming potential measurements can be carried out with solids of any shape. Therefore, column packings can be characterized as they are used in the applications. A few relatively complex streaming potential devices have been developed within the past several years in an attempt to decrease analysis time and improve data acquisition [35–39]. For systems of membranes, capillaries, and flat plates where sample equilibration time can be quite short

these devices are fairly efficient [40]. Packed capillary columns, however, with stationary phases of granular or monolithic nature for μ-HPLC and CEC require utilization of high flow velocities/high pressures due to their high surface area.

## 3. Experimental

### 3.1. Materials

The electrolyte solutions contained 0.001 *M* sodium or potassium chloride of different pH values. For the calculations of the zeta potential, Reynolds number and specific permeability, the data for these electrolytes were taken from the literature as those for water at 25°C [41]: viscosity of the electrolyte solutions was 0.001 kg/m per s, the dielectric constant $695\times10^{-12}$ F/m and the density 1000 kg/$m^3$. The specific conductance, $\lambda$, of the electrolytes was measured by a Digital Conductivity Meter, Traceable™ (Fisher Scientific, Fairlawn, NJ, USA). Additionally, 5 m*M* sodium phosphate buffers, pH 3, with 50 m*M* NaCl and different concentrations of acetonitrile were also employed.

Water was taken from a Milli-Q water purification system (Millipore, Bedford, MA, USA), with a specific resistance of $>10^7$ ohm cm. Dimethyl sulfoxide (DMSO) was purchased from Burdick & Jackson (Muskegon, MI, USA), styrene from Fluka (Ronkonkoma, NY, USA), divinylbenzene (DVB) (85%) and vinylbenzyl chloride (VBC) from Dow (Midland, MI, USA), and azobisisobutyronitrile (AIBN) (98%) from Pfaltz & Bauer (Waterbury, CT, USA), γ-(trimethoxysilyl)propyl methacrylate from Polysciences (Warrington, PA, USA), 2,2-diphenyl-1-picrylhydrazyl hydrate (DPPH) from Aldrich (Milwaukee, WI, USA), hydrofluoric acid (48%) was of analytical reagent grade from Mallincrodt (Paris, KY, USA); 1 N and 0.1 N hydrochloric acid and sodium chloride were from J.T. Baker Inc. (Phillipsburg, NJ, USA). Fused-silica capillaries 50 and 75 μm I.D. and 375 μm O.D. with polyimide cladding were purchased from Quadrex (Woodbridge, CT, USA). Styrene and DVB were washed with 10% (w/v) aqueous sodium hydroxide to remove the inhibitors before use. The toluene and acetone were anhydrous and stored over dehydrated molecular sieves (Type 4A, 8–12 mesh, Fisher Scientific Co., Fair Lawn, NJ, USA).

### 3.2. Column preparation

The chemistries employed in the preparation of the column used in the experiments are illustrated in Figs. 1 and 2. In Fig. 3, the typical scanning electron micrographs of the open and packed fused-silica capillary columns are presented. A brief description of the monolithic support, which is functionalized to form the chromatographic surface, is given below.

The innerwall of the fused-silica capillary (Column I) was silanized (Column II) with a solution of 50% (v/v) γ-(trimethoxysilyl) propyl methacrylate and 0.01% (w/v) DPPH in DMF. After both ends of the capillary were sealed, it was heated at 120°C for 6 h in the oven. Capillary columns with monolithic stationary phase were prepared from silanized fused-silica capillaries by in situ copolymerization of divinylbenzene either with styrene or vinylbenzyl chloride in the presence of a suitable porogen. The method described in the literature [16] for the monolith preparation was used throughout the study. The characterization of the columns by the permeability, conductivity, porosity under HPLC and CEC conditions is described in the same reference [16].

The monolithic column was functionalized in situ by reacting poly(vinylbenzyl chloride-*co*-divinylbenzene) porous support either with dimethyloctylamine (Column VI) or dimethyldodecylamine (Column VIII) overnight. The chromatographic surface thus obtained maintained $C_8$ or $C_{12}$ alkyl chains and positive charges. Column packings with strong negative charges were obtained by treating the porous matrix with chlorosulfonic acid for 20 min (Column VII). Also fluid impervious poly(styrene-*co*-divinylbenzene) coating (Column III) [42], porous monolithic (Column V) and poly(vinylbenzyl chloride-*co*-divinylbenzene) PLOT (Column IV) columns were characterized here. In some experiments, a column packed with non-endcapped octadecylated (ODS) 5-μm silica particles (Column IX) was also tested.

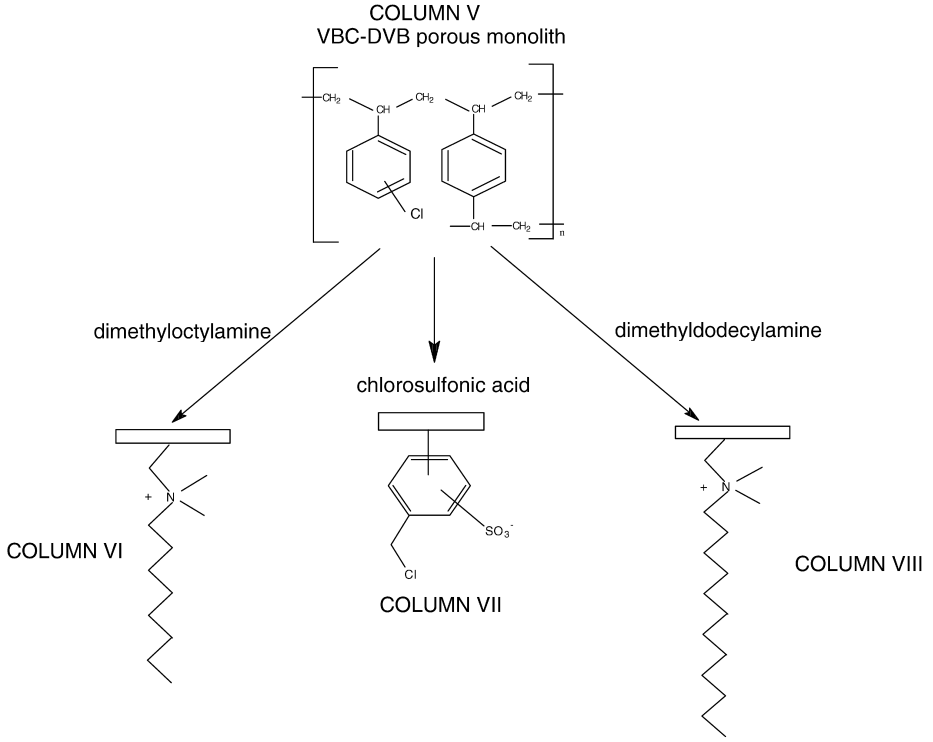


Fig. 2. Functionalization of the support.

### 3.3. Electrokinetic measurements

#### 3.3.1. Streaming potential

##### 3.3.1.1. Design criteria for measuring apparatus

From Eq. (3), it is evident that the apparatus for measuring streaming potentials must include means for measuring the voltage generated, the pressure, which drives the fluid flow, and the specific electrical conductivity of the electrolyte solution. The electrical resistance of the packed capillary columns is high. Therefore, an electrometer with a large internal resistance must be used for measurements of the streaming potential. We found that an electrometer with internal impedance greater than $10^{14}$ Ω can be used to measure the streaming potential in columns. It is necessary to use a high pressure metering pump with packed capillary columns of low specific permeability (0.01–0.5 D). High pressure also allows carrying out electrokinetic investigations in a wide range of operating conditions and even at high electrolyte concentrations that are often employed in capillary electrochromatography.

##### 3.3.1.2. Electrodes

The electrodes are arguably the most important parts of the experimental set-up. At high salt concentrations and/or with low pressure drop the streaming potentials are small, on the order of mV. Drift and other spurious effects at the electrodes may make the accuracy of the measurement questionable. It is better to use non-polarizable electrodes [20], e.g. $Cu–CuSO_4$, calomel ($Hg–Hg_2Cl_2$), $Pb–PbSO_4$, or Ag–AgCl. Of these the Ag–AgCl electrodes appear to be the most suitable. The silver–silver chloride electrode can be manufactured in the form of a solid electrode by electrolyzing a piece of silver in a solution containing chloride ions. The other electrode types contain a fluid electrolyte and make contact with the sample through a porous membrane that has two disadvantages in that the electrolyte from the electrodes may contaminate the sample and the electrodes cannot generally withstand pressure. The

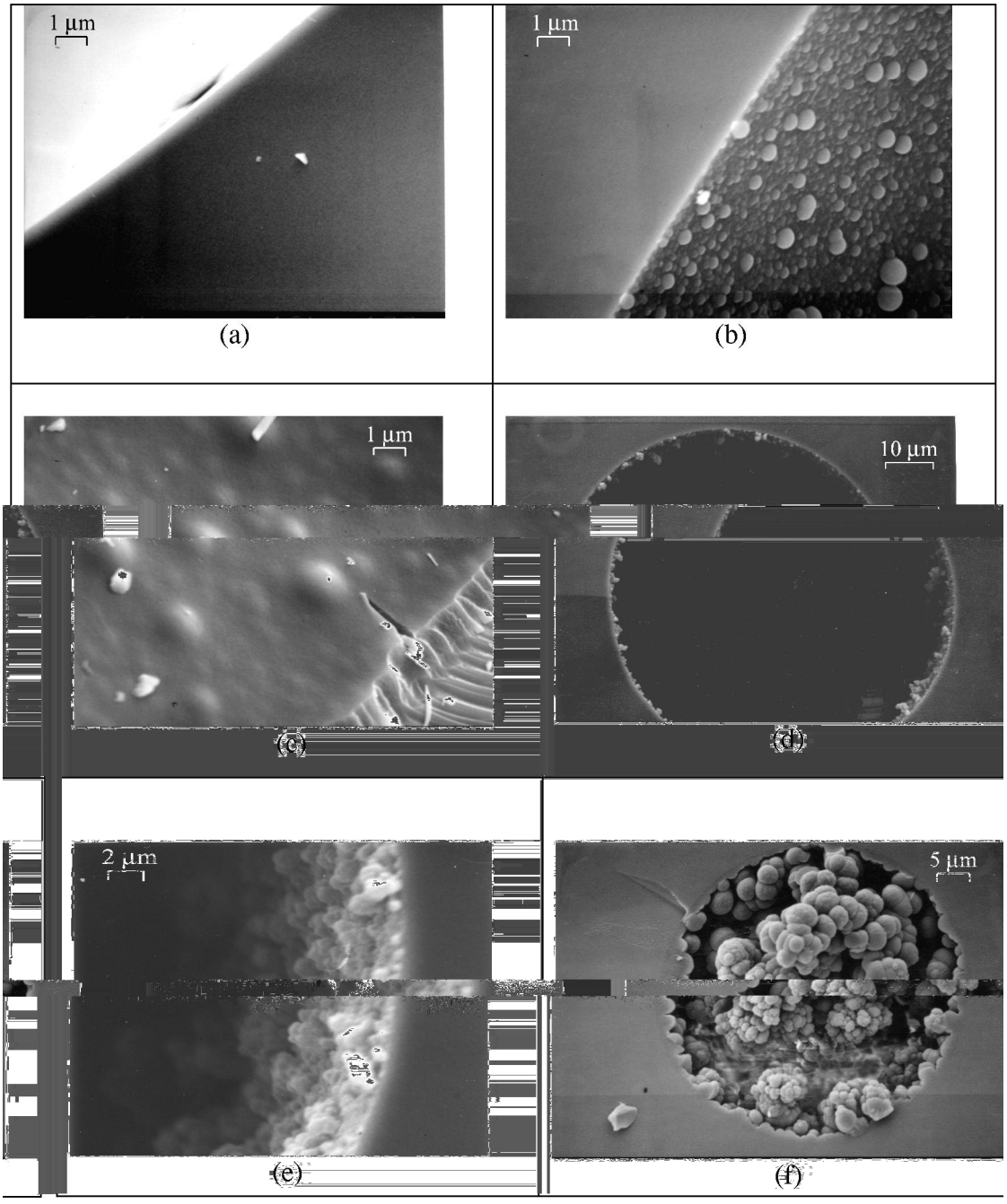


Fig. 3. Typical scanning electron micrographs of the open and packed fused-silica capillary columns. (a) Enlarged lumen of the raw fused-silica capillary, Column I, 50 μm I.D.; (b) enlarged lumen of the fused-silica capillary with nonporous polystyrene coating, Column III, 75 μm I.D.; (c) enlarged lumen of the porous layer open tube (PLOT) column, poly(VBC-DVB) coating, Column IV, 75 μm I.D.; (d) cross-section of PLOT column; (c) cross-section of PLOT column at higher magnification than in (d); cross-section of poly(VBC-DVB) monolith, Column V, 50 μm I.D.

Ag–AgCl electrode is user-friendly, quite rugged, and easy to manufacture. Therefore it is engaged in most recent laboratory investigations [40,43–47] on streaming potential.

The potential electrodes used in this work were solid Ag–AgCl electrodes, prepared by electrolyzing a high purity silver wire of dimensions 0.5×1 mm, Part No. Ag005150/21 (Good Fellow, Cambridge, UK) in 1 *M* HCl solution. The low noise and stability of the electrodes were checked by an over 2-h long measurement of the potential difference between a pair of Ag–AgCl electrodes placed in a 10 m*M* solution of NaCl in deionized water. The drift in this experiment was approximately 3 mV. After about 20–30 min, the electrodes appeared to be stabilized and during the remaining time of the experiment, drift is well below 1 mV. All streaming potential measurements described in this work were made with a stabilization period of at least 20 min, and thus any influence of electrode drift on measurements should be small. The use of reversible silver chloride electrodes with a low potential of the asymmetry makes it possible to move into the region of high concentrations of the electrolyte, where the zeta potentials are small. The electrodes were stored in deionized, distilled water after each use and cleaned when required by 30-s immersion in 30% nitric acid solution. The electrodes were regenerated once a week.

*3.3.1.3. Description of the streaming potential apparatus*

A schematic illustration of the apparatus used for generation and measurement of streaming potential is shown in Fig. 4. The instrument comprises a micro flow syringe pump (1) Model SFC-500 Micro Flow Pump (Isco, Inc., Lincoln, NE, USA), dual channel chart recorder (2) Model BD 41(Kipp & Zonen, Delft, The Netherlands) for simultaneous monitoring both the streaming potential and the inlet pressure of the column under investigation and a high-impedance (greater than $10^{14}$ ohm shunted by 22 pF) Model 610B Electrometer (3) (Keithley Instruments, Inc., Cleveland, OH, USA). The capillary (4) was mounted between two electrolyte-filled PEEK crosses having 17.2 μl internal volume each, Part No. P-730 (Upchurch Scientific, Oak Harbor, WA, USA). The capillary column (4), pump (1) and waste (5)

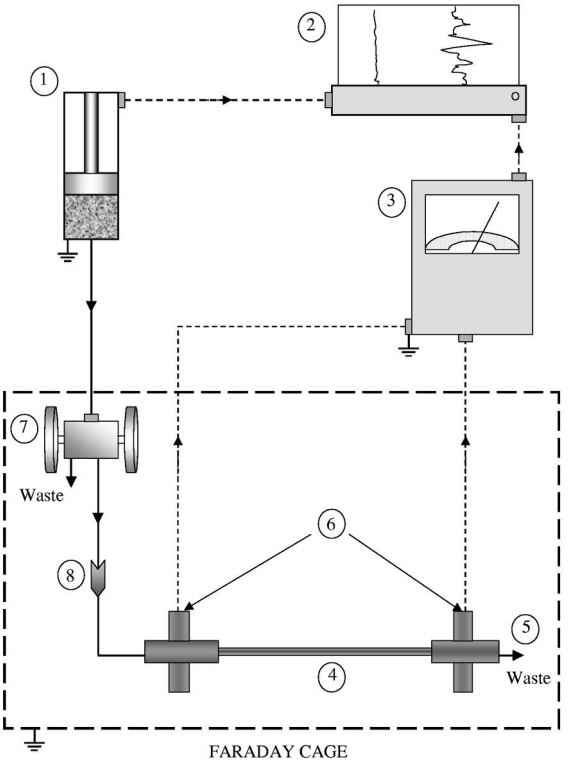


Fig. 4. Schematic diagram of the experimental set-up.

lines were connected to the horizontal ports of the crosses. The silver–silver chloride electrodes (6) were placed at the vertical ports.

The 50-ml capacity syringe pump was used to generate flow in the range of 0.02–600 μl/min with maximum pressure of 690 bar. The pump was operated in constant pressure mode, producing pulse-free flow and measuring the driving pressure. Electrolyte solution was forced to flow from the pump into and through a measuring cell and to waste. Throughout the experiments, the unit was placed in a Faraday cage, to decrease the effect of extraneous electromagnetic fields.

*3.3.1.4. Measurement of streaming potential and data handling*

In streaming potential measurements, first the pH and temperature of the electrolyte were read. Then the cell was assembled with the capillary column in place and the system was flushed at maximum pressure of 250 bar to remove entrapped air. Upon

attainment of a steady state, the corresponding streaming potential was recorded. Afterwards the pressure in the measuring cell was released by opening the high pressure Dual-stem valve (7) in Fig. 4, Cat. No.06-653-112D (SSI, State College, PA) to the atmosphere. Data points were collected by increasing pressure stepwise in 50-bar increments with the step conditions lasting 30 min allowing enough time to reach an equilibrium (according to experimental observations). Since the kinetics of equilibration between the electrolyte solution, the electrodes, and the stationary phase has the impact on measurement uncertainty, operating with a continuously changing pressure (flow) is not recommended [48], even though it is the standard operating mode of some commercially available instruments. The measurements were carried out at ambient temperature as it was previously found [49,50] that zeta potentials depend only weakly on temperature. The temperature dependence of the viscosity and dielectric constant was accounted for in all calculations.

### *3.3.2. Electrosmotic flow*

The CEC experiments were carried out in a home-made apparatus, equipped with a model Spectra-FOCUS detector and a Model 9550-0155 on-column capillary cell (Thermo Separation Products, Fremont, CA, USA) [16]. In order to keep the zero voltage at the column detection side, the outlet electrode was grounded. The 30 kV bipolar power supply (Spellman, Plainview, NY, USA), connected to the inlet electrode, allowed for a reversible polarity.

The samples were injected electrokinetically for 2 s at a voltage of 2 kV. If not otherwise stated, separation was performed at an applied voltage of 15 kV with anodic EOF for packed monolithic columns with quaternary ammonium groups at the chromatographic surface and cathodic EOF for all other columns. Between runs, the column was rinsed with the mobile phase for 10 min at 8 bar inlet pressure. All experiments were carried out at room temperature and both inlet and outlet of the column were kept at atmospheric pressure.

### *3.3.3. Accuracy and reproducibility*

The relationship between streaming potential and a driving pressure responsible for the flow of 1 m*M* KCl, pH 4.0, electrolyte solution was examined first. In order to avoid artifacts resulting from the presence of other ions, particularly at low electrolyte concentrations, buffers were not used in preliminary studies. Fig. 5 shows the dependence of the streaming potential on the pressure difference of the above electrolyte. The solid and open circles were obtained by increasing and subsequently lowering the pressure. Apparently, there is no hysteresis and the data are well reproducible with standard deviation lower than 5%. Up to 300 bar, the plot of the streaming potential against the pressure is linear, with $R^2 = 0.995$. According to the Helmholtz–von Smoluchowski theory, such linearity is expected in the behavior of the $\zeta$-potential. The day-to-day reproducibility of the streaming potential measurements was satisfactory. As can be inferred from Fig. 6, $\zeta$-potential and specific permeability values of the two measurements made about 1 week apart on porous styrenic unfunctionalized monolith, Column V, are $-4.9$ and $-4.7$ mV, and 0.572 and 0.574 D, respectively in 1 m*M* KCl solution at pH 4.0. The standard deviations within 1 day and between data collected 1 week apart are of the same order of magnitude.

It was found that equilibration of freshly prepared columns was rather slow in our system and with an applied pressure of 250 bar on about a 30-cm

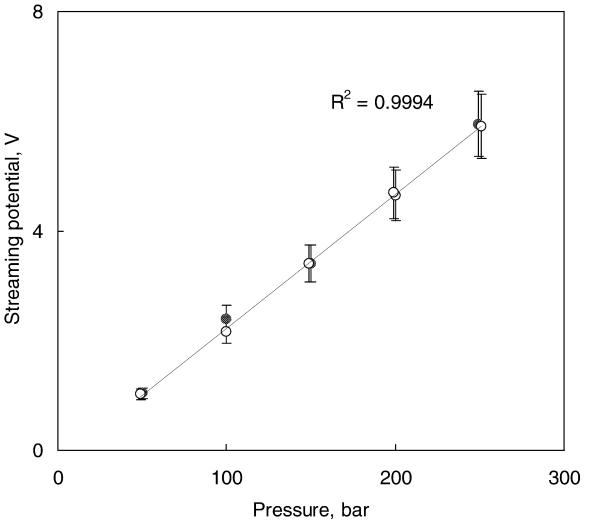


Fig. 5. Dependence of the streaming potential on the pressure difference in 1 m*M* KCl solution. The open and solid circles indicate an increase and a subsequent lowering of the pressure.

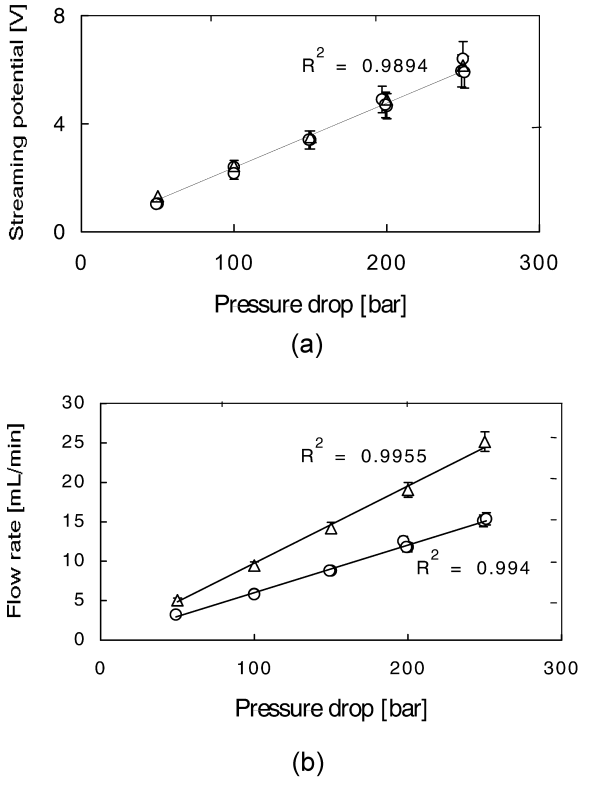


Fig. 6. The day-to-day reproducibility of the (a) streaming potentials and (b) the column permeability were measured with Column V. This column had a porous styrenic monolithic packing without functionalization. Eluent, 1 m*M* KCl solution, pH 3.5, conductivity 0.225 mS/cm.

monolithic column had taken 1–3 h. Such extended column equilibration time is not unusual in chromatography [51] and can be due to slow solute diffusion either toward or away from the solid surface throughout, adsorption of potential determining ions or limited dissolution of the surface [52]. All measurements of streaming potential were carried out after the column was equilibrated.

In CEC mode, a freshly made column was always equilibrated with the mobile phase overnight. Later, when a different mobile phase was introduced, the column was rinsed for ca. 3 h by applying nitrogen gas pressure of 8 bar at the inlet vial, and then equilibrated electrokinetically at 5 kV for 30 min or until the attainment of a stable base line. To prevent a decrease in the electrosmotic velocity observed during long time usage of bare fused-silica capillaries and to obtain a higher reproducibility within 1 day, the following procedure was adopted [32]. A ''fresh'' surface was established every morning by rinsing the capillary first with 1 *M* HF for 30 s (about 10 μl); after a washing step with distilled water, the capillary was rinsed with 1 N NaOH for 5 min (about 100 μl) and then with the respective electrolyte for another 5 min. In order to prevent the formation of a gel layer overnight, the capillary was dried by aspirating it at the end of the day. In between measurements no rinsing with NaOH was carried out. Because of the low buffering capacity, the electrolyte vessels were filled with fresh electrolyte after each run, as it was observed that the pH could change by several units when the same electrolyte solution was used for several consecutive measurements. For all the capillaries, each EOF measurement at the different pH values was performed in triplicate. The high-voltage power supply unit was operated in the constant-voltage mode at 15 kV.

In this work, the term $\zeta$-potential is used for the $\zeta$-values calculated from Eqs. 3 and 4 with correction factor equal to unity. These values are frequently referred to in the literature [20] as ''apparent zeta potential''.

## 4. Results and discussion

Fig. 7 illustrates typical dependence of the streaming potential on the applied pressure determined with 1 m*M* NaCl, pH 5.54, in an open (a) and packed (b) capillary. As seen, plots of streaming potential versus pressure drop across the column are nearly straight lines as predicted by Eq. (3). The linear correlation coefficients for these data were always better than 0.995, indicating that we were working in the laminar flow regime. The highest Reynolds numbers were about 3.8 for packed and 350 for open capillaries. That the flow is not turbulent is shown by the linear dependence of the streaming potential on the applied pressure [53,54]. In Fig. 7, the lines do not always pass through the origin and this behavior is attributed to parasitic electrochemical reactions at the electrodes [55]. However, this phenomenon does not affect the value of the $\zeta$-potential which is proportional to the slope of the linear regression lines according to Eq. (3).

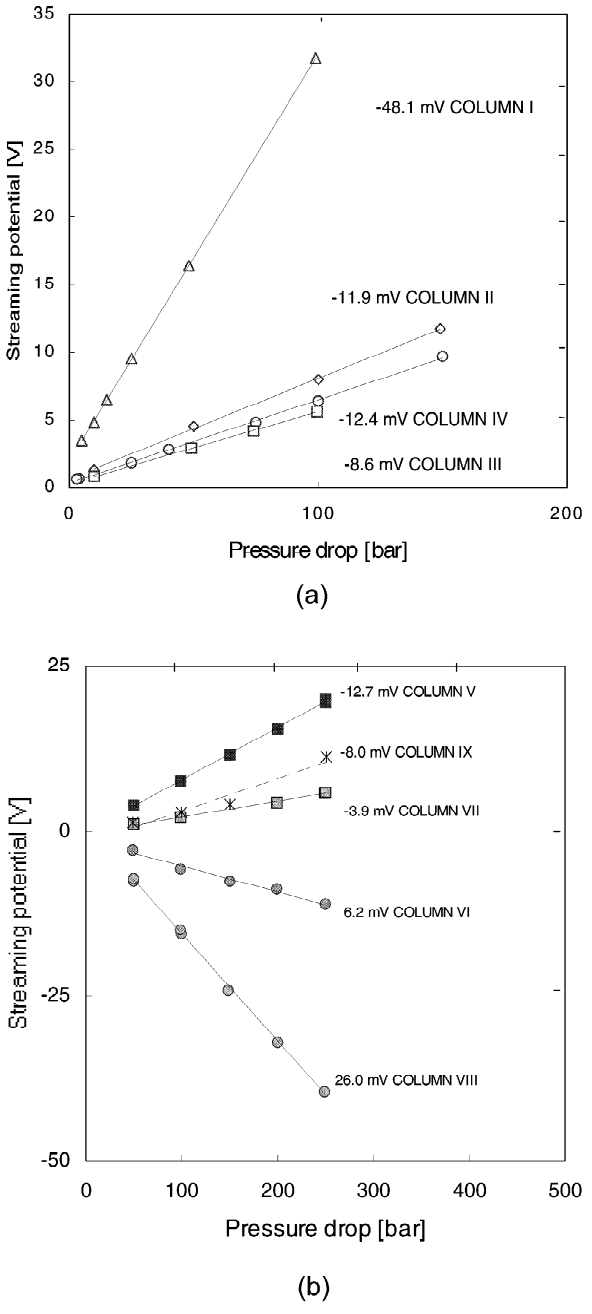


Fig. 7. The variation of streaming potential with applied pressure in 1 m*M* NaCl, pH 5.54 for (a) packed and (b) open tube capillaries.

In the experiments, the ionic strength of the electrolytes was either 1 or 50 m*M*. Therefore the von Smoluchowski equation with correction factor of unity [56] was applicable since the double layer thickness was much smaller than the diameter of the open capillary or the pore diameter. In the calculations of the $\zeta$-potential, the conductivity of the electrolyte in the pores was taken as being equal to that of the bulk mobile phase. It is noted that, according to Ref. [20] the surface conductance becomes significant for plugs and diaphragms only at concentrations below 1 m*M*.

### *4.1. Effect of pH on zeta potential*

Fig. 8 shows plots of the $\zeta$-potential of packed and open fused-silica capillaries against the pH of the 1 m*M* NaCl solution.

#### *4.1.1. Open capillaries*

The fused-silica tubings were either raw or functionalized at the inner wall. To explain the results shown in Fig. 8a, let us consider first the data obtained with raw fused-silica capillary (Column I). In this case the $\zeta$-potential changes from $+30$ to $-60$ mV when the pH increases from 2.0 to 9.0. The pH-profile of $\zeta$-potential has a sigmoidal shape with an inflection point at about pH 4.0. This is readily explained by the protonation/deprotonation of the silanol groups at the surface of the raw fused-silica capillary [57,58].

For the sake of comparison, $\zeta$-potentials ($\Delta$) obtained from streaming potential data using a commercially available electrokinetic analyzer Model EKA (Anton Paar GmbH, Graz, Austria) on clear quartz sand in 1 m*M* KCl solution [59] are also illustrated. It is seen that the pH dependence of $\zeta$-potential of quartz sand and that of quartz capillary are quite similar. This observation gives further support to the usefulness of our instrument. Furthermore, both quantitative and qualitative behavior of quartz capillary tube shown in Fig. 8a agree well with literature data obtained by measurement of streaming potential with quartz–water systems [34,60].

In order to enhance the adhesion of the porous monolith to the inner surface of the silica capillaries, their inner wall was treated with $\gamma$-trimethoxysilyl

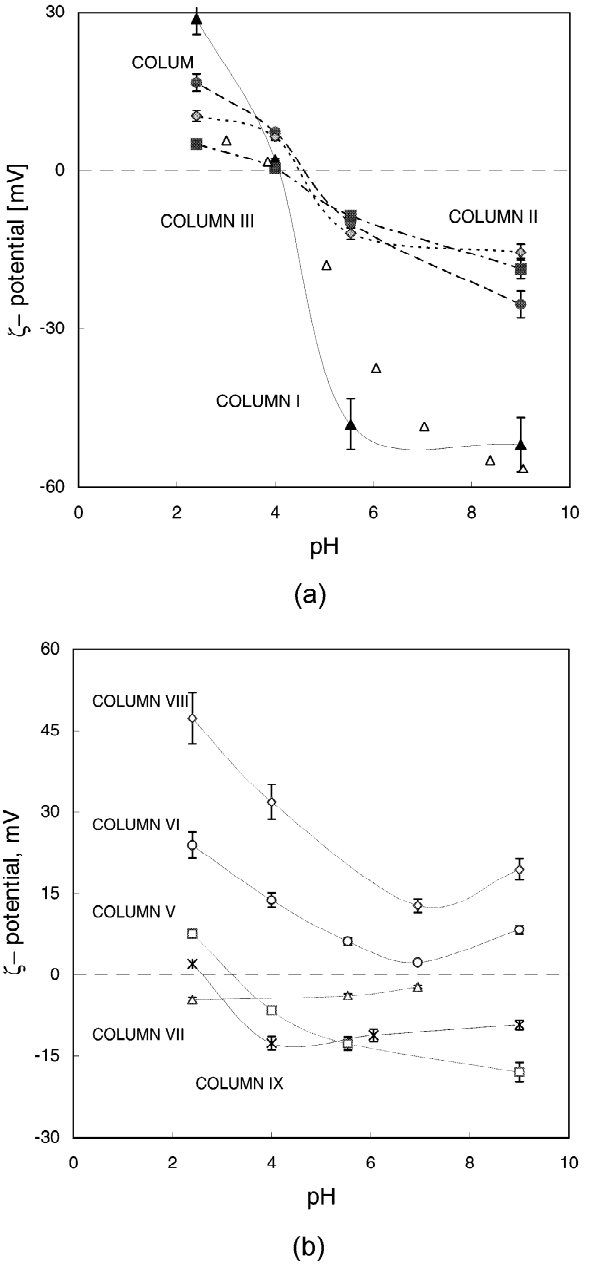


Fig. 8. pH profile of zeta potential in (a) open tube (solid symbols) and (b) packed columns (open symbols) in 1 m*M* NaCl. Data (Δ) from Ref. [59] obtained by streaming potential measurements with EKA instrument on clear quartz sand in 1 m*M* KCl solution are included in (a) for comparison.

propyl methacrylate, a heterobifunctional silanizing agent. The quality of silanization was evaluated by measuring the wetting properties of the capillary using the capillary rise method [16]. Satisfactory treatment resulted in a contact angle in water of about 75° in comparison to the contact angle of 25° obtained with raw fused-silica capillary (Column I). As seen in Fig. 8a, silanized fused-silica capillary, Column II, exhibits a relatively small negative $\zeta$-potential at alkaline pH. The data show that successful silanization results in a drastic decrease in the $\zeta$-potential of the wall to a value commensurate to that of nonporous PS–DVB coating (Column III) which has a contact angle in water of about 120° [42]. Marked differences in the $\zeta$-potentials of unmodified and modified silica surfaces are observed at pH below and above the inflection point. At pH$>$5.0, the zeta potential of silanized silica is smaller for the unfunctionalized one due to the decreased density of silanol groups on the modified silica surface.

Polymer-coated capillaries with no ionogenic groups exhibit quite different behavior. The plots of $\zeta$-potentials measured with Columns III and IV against pH suggest that the surfaces are negatively charged at high pH and slightly positively charged at low pH. This is most likely due to adsorption of $Cl^-$ or $OH^-$ anions and $H^+$ or $Na^+$ cations from the contacting solution. It is known that the strong specific adsorption of the halide anions ($Cl^-$) gives rise to an appreciable negative surface potential at low electrolyte concentrations [45]. In the case of a nonpolar surface with no fixed charges, the affinity of hydrated ions to the neutral surface can be different so that one kind of ion binds more strongly to the surface than another [20,61]. Measuring the pH dependence of the $\zeta$-potential of two open tubular columns with a hydrophobic styrenic nonporous (Column III) and a porous (Column IV) surface we have found that the plots exhibit no plateau. The increase in absolute values of the $\zeta$-potential at both high and low pH is caused by adsorption of hydroxyl ions or protons at the chromatographic surface.

### *4.1.2. Packed capillaries*

The pH dependence of the $\zeta$-potential has also been investigated with columns having porous monolithic packing which were functionalized by different

methods. The results are presented in Fig. 8b by plotting the $\zeta$-potential against the pH of a 1 m*M* NaCl solution. Column V which was packed with an unfunctionalized porous poly(styrene–divinylbenzene) monolith shows the behavior typical for non-polar surfaces with no fixed ionic groups, that have an isoelectric point in the neighborhood of pH 4.0. With such surfaces the zeta potential versus pH plot does not plateau as was illustrated before in Fig. 8a with coated fused-silica capillaries (Columns III and IV).

Adsorption sites on the unfunctionalized styrenic surface are likely to have this origin from unreacted double bonds [46]. This is supported by reports in the literature [62] that polystyrene latex with no emulsifier and no titratable ionic groups can have a relatively high negative $\zeta$-potential of about 50 mV. Such phenomena were also observed with various hydrocarbonaceous surfaces and were explained by ''injection of electrons'' from water into polymeric surfaces [62].

In the case of polymers with alkylaminated surfaces bearing dimethyl octyl ammonium (Column VI) or dimethyl dodecyl ammonium (Column VIII) functional groups on poly (vinylbenzyl chloride-divinylbenzene) porous monolithic column packings, the $\zeta$-potential is positive in the entire pH range. As shown in Fig. 8b, the $\zeta$-potential decreases and goes through a minimum at about 3 mV with Column VI and about 13 mV with Column VIII. The decrease in the $\zeta$-potential is likely due to the amphiphilic nature of the chromatographic surface, at which quaternary ammonium functions are fixed at the hydrophobic surface of the styrenic support. Thus, electrostatic heterogeneities [63] can engender a decrease in $\zeta$-potential due to an increase in the negative $\zeta$-potential of the styrenic surface with increasing pH (as seen with Column V). Columns with such surfaces were found to exhibit low column efficiency in the separation of basic proteins and peptides at neutral pH by capillary electrochromatography (results not shown). The column efficiency was improved, however, upon addition of salt; thus, poor column performance was most likely due to electrostatic attraction of the basic solutes by negatively charged polymeric support. The dependence of the $\zeta$-potential on pH indicates that at low pH higher electrosmotic flow is to be expected.

The behavior exhibited by Column VIII and Column VI in Fig. 8b might be explained by the effect of the different alkyl chain length of the quaternary ammonium functions. The $C^{13}$ NMR studies on *n*-alkyl-silica [64] showed that octyl chains are more disordered than the self-assembling ''crystalline'' dodecyl chains due to weaker van der Waals interactions between the intermediate-length alkyl chains. In turn, the surface density of the chains is higher for monolithic columns functionalized with quaternary ammonium dodecyl groups. Thus the surface charge density becomes higher as presented schematically in Fig. 9. In addition, longer alkyl chains create a microenvironment that increases the basicity of the head amino group [65]. This further increases the effective charge density and results in the higher $\zeta$-potential shown by the data obtained with Column VIII. These results suggest that the monitoring of the streaming potential can be helpful in the optimization of the steps of surface treatment and as a tool for quality control of fused-silica capillary columns.

A typical pH profile of $\zeta$-potential of weakly acidic surfaces is illustrated in Fig. 8b by the performance of Column IX, which is packed with octadecylated silica. The $\zeta$-potential at low pH is positive, probably due to the adsorption of $H^+$ ions at the silica surface. This phenomenon was also mentioned in view of Fig. 8a with regard to the pH dependence of the $\zeta$-potential in raw and silanized fused-silica capillaries. As shown in Fig. 8b, the $\zeta$-potential becomes more negative as acidic groups start to dissociate and plateaus when they reach a fully dissociated state.

Column VII was prepared by sulfonating the monolithic support to obtain strongly negative $\zeta$-potential even at low pH values. Nevertheless, as

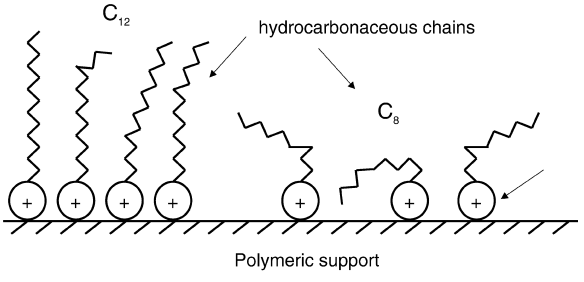


Fig. 9. Illustration of the hypothetical differences in the surface structure of stationary phases with dodecyl dimethyl and octyl dimethyl ammonium functions adopted from Sindorf et al. [64].

shown in Fig. 8b, Column VII exhibits a more or less stable $\zeta$-potential across the practical pH range albeit its value is rather low.

### 4.2. Zero charge conditions

In capillary electrochromatography it is often required to know the conditions for zero charge. According to von Smoluchowski Eq. (4), the electrosmotic flow ceases at zero $\zeta$-potential. However, the establishment of no-flow conditions is difficult within the electrosmotic measurement context as the alteration of EOF in the neighborhood of zero EOF velocity requires a prolonged elution time of a tracer and renders the measurement tedious. As could be gleaned from Fig. 10, the elution time of DMSO in Column I was 5 min at pH 9.0 and 21 min at pH 4.0. Furthermore, the required polarity of the electric field in CEC instrument should be known in advance. In contradistinction, in streaming potential measurements this information can be determined instantaneously, since the voltmeter shows the sign and the value of the streaming potential upon applying the pressure gradient to the chromatographic column.

The double layer properties can be characterized by the surface charge density, point of zero charge, zeta potential and isoelectric point. The zero charge condition reflects the acidic or basic nature of the surface and can be expressed by the point of zero charge (pzc) and isoelectric point (i.e.p.). Point of zero charge corresponds to zero surface charge density and reflects the affinity of the surface under investigation for charge-determining ions and is therefore a surface characteristic. The isoelectric point, which is the electrokinetic counterpart of the pzc is the pH where the $\zeta$-potential is zero. If no specific adsorption of ions occur, the pzc and i.e.p. coincide.

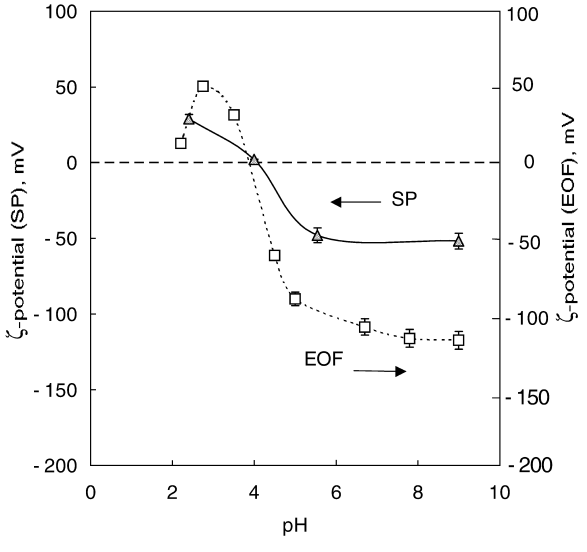


Fig. 10. Zeta-potential evaluated from the electrosmotic flow (open symbols) and the streaming potential (solid symbols) in raw fused-silica capillary, Column I, against the pH of the mobile phase in 1 m*M* NaCl.

As seen in Fig. 8, the i.e.p., determined at an intersection of the $\zeta$-potential curve with pH axis for the silanized and raw fused-silica capillaries, is about pH 4.0, and about pH 2.5 for octadecylated silica column packing which is in good agreement with previously reported values [6,20]. For Columns III, IV and V, the inflection points of the curves are in the pH range from 3.5 to 5.0 which agrees well with results published for polymeric surfaces [66]. This pH value, typical for the p$K_a$ value of aliphatic carboxylic acids, was explained by the presence of carboxylate groups, originating from the production process.

### 4.3. Zeta potential determined from streaming potential and electrosmotic measurements

It is generally accepted that the theory is valid if it yields the same zeta potential measured by different electrokinetic methods at the same surface. Yet, such *electrokinetic consistency* [63], was not satisfactorily achieved to date [67–74].

Our results of a systematic study on the dependence of the $\zeta$-potential on pH are shown in Fig. 10. The $\zeta$-potentials were obtained in a 50 μm I.D. raw fused-silica capillary with 1 m*M* NaCl solution by two methods. The $\zeta$-potential values from electrosmosis data were generally higher than those obtained from streaming potential measurements in the pH range from 2.5 to 9.0. When the pH is equal to the isoelectric point, the data obtained with a given fused-silica capillary are the same, within experimental error.

As expected and shown in Fig. 10, at the pH above i.e.p., the $\zeta$-potential is negative due to

deprotonation of the surface hydroxyls. There is a plateau in the zeta potential–pH curves obtained by both methods above pH 5.5. This plateau manifests the completion of the dissociation of the silanol groups. At very low pH, the positive $\zeta$-potential, as measured by both methods, drastically decreases. This could be explained by high HCl concentration needed to obtain corresponding pH value, and thereby the increased ionic strength ($\lambda = 1.0$ mS/cm at pH 2.5 vs. about 0.12–0.18 mS/cm in the pH range 3.0–9.0) of the electrolyte with concomitant decrease in the double layer thickness.

Quantitative discrepancies found between the results of these two methods can be explained by the indirect character of the $\zeta$-potential measurements [75]. Indeed, both methods studied differ in the way of coupling the $\zeta$-potential and the relative motion of the fluid with respect to the charged surface. Furthermore, in electrosmosis, data on temperature inside the capillary and therefore its influence on $\zeta$-potential via viscosity and mobility are not available. Temperature excesses in the range from 40 to 70°C with concomitant decrease in the viscosity and the dielectric constant of water are well known in CE systems [76,77]. Thus, the $\zeta$-potentials obtained by both methods could be brought into an agreement by setting the temperature to $T = 88$°C in Eq. (4). However, such adjustment seems unrealistic in a 50-μm I.D. capillary with 1 m*M* NaCl in 20 000 V/m electrical field strength and a liquid cooling system employed in a Beckman PACE 2000 instrument which was used for experiments with open capillaries. Calculation of the temperature increase in the above system [77] suggests that $T$ may increase by less than 1°.

Szymczyk et al. [78] put forward the hypothesis that the observed differences could be caused by a shift in the location of the shear plane within the electrical double layer. This would imply that the $\zeta$-potential would relate to flow conditions at the solid–liquid interface. The two methods outlined above employ different flow fields: laminar flow with parabolic flow profile in the case of streaming potential and plug flow profile in the case of electrosmosis. Under these circumstances, the analogy of Stern layer potential and $\zeta$-potential is no longer valid. The observed variations between $\zeta$-potential numeric values could then be due to the shift of the shearing plane within the electrical double-layer under different flow conditions. In order to quantitatively estimate a value of the shift in the shear plane location, $\delta$, let us rewrite Eq. (2) introducing $\zeta_1$ and $\zeta_2$ as the potentials at the shearing planes, located at the distance $x_1$ and $x_2$ from the Outer Helmholtz Plane (which is a borderline between the inner part of the diffuse layer and its outer or mobile part) for the electrosmotic and streaming potential measurements, respectively, as follows:

$$\delta = x_1 - x_2 = \frac{1}{\kappa}\left\{ \ln \frac{\tanh\left(\frac{-ze\zeta_2}{4kT}\right)}{\tanh\left(\frac{-ze\zeta_1}{4kT}\right)} \right\} \quad (5)$$

where for 1 m*M* NaCl electrolyte solution at 25°C, $1/\kappa = 9.61$ nm [61]. In our calculations, the value of the shift in the location of the shearing plane equals zero at the isoelectric point and increases with pH to a maximum value of 5 nm at pH 9.0 as shown in Fig. 11. It was reported [26], that the distance between the slipping-plane and the interface was calculated in the range from 1 to 10 nm for different electrolyte

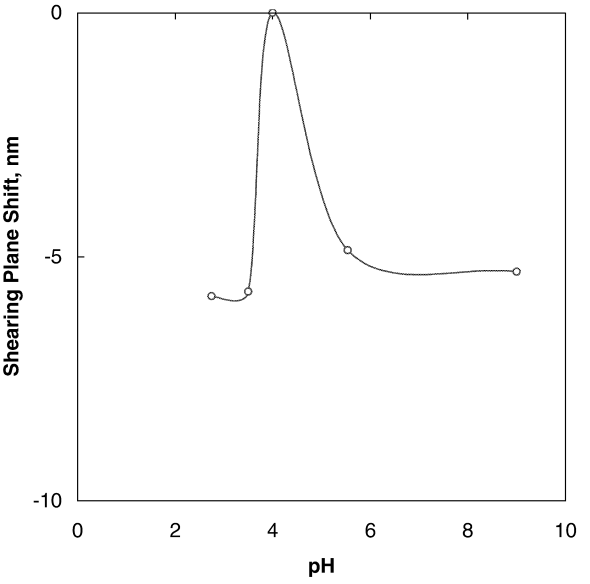


Fig. 11. Shift in the shear plane location evaluated from the electrosmotic flow and the streaming potential in raw fused-silica capillary, Column I, against the pH of the mobile phase in 1 m*M* NaCl.

concentrations. These results are in the range of our calculations.

In addition to open fused-silica capillaries, packed capillaries with *amphiphilic* stationary phases having ionogenic functions and chromatographic binding sites were employed for comparison of the two methods. In Fig. 12, $\zeta$-potentials evaluated from the electrosmotic flow and the streaming potential in monolithic octylaminated, Column VI, and dodecylaminated, Column VIII, polystyrene columns are presented. Hydro-organic mobile phases containing acetonitrile and 5 m*M* sodium phosphate buffer, 50 m*M* NaCl, pH 3, were employed. The dependence of streaming potential on $\Delta P$ was linear for the buffers studied, confirming the laminar character of the flux through the packing. Hence, the conversion of streaming potential into $\zeta$-potential was possible using Eq. (3) which implies this type of flow. As seen in Fig. 12, for both $C_8$ and $C_{12}$ columns the magnitude of the $\zeta$-potential determined from the electrosmosis was generally greater than that from streaming potential with the smallest difference at 50% ACN. This agrees well with data reported by Mukhtar et al. [73] for polymeric membranes.

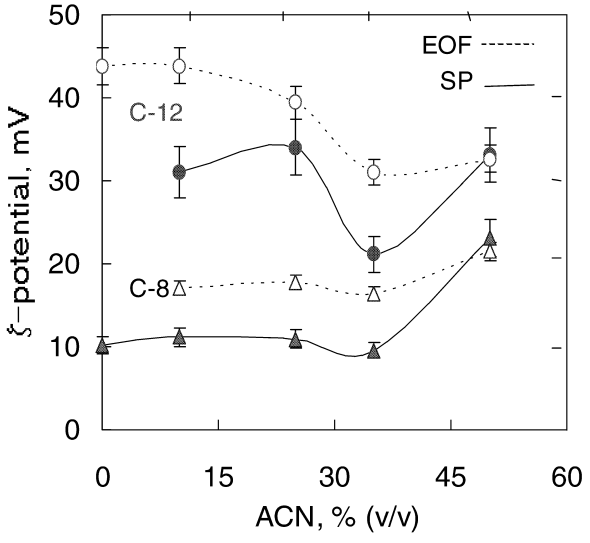


Fig. 12. Zeta-potential evaluated from the electrosmotic flow (open symbols) and the streaming potential (solid symbols) against the acetonitrile concentration in monolithic octylated, Column VI, and dodecylated, Column VIII, polystyrene columns in 5 m*M* phosphate buffer, 50 m*M* NaCl, pH 3.0.

It appears that each method allows the determination of the zeta potential of the tested materials with a good qualitative agreement between the two methods. They both give the same value for the isoelectric point for open fused-silica capillaries, the same curve profiles of $\zeta$-potential versus pH and acetonitrile concentration. As a result, each method brings the same information concerning the nature of the surface ionizable functions. This is important since such functions have a strong impact on EOF, stationary phase selectivity, etc. Indeed, long distance electrostatic interactions, as well as short-range acid–base interactions [79], originate from the presence of ionizable groups at the surface.

#### *4.3.1. Effect of acetonitrile environment on zeta potential*

Stationary phases in CEC columns are ''bona fide'' ion-exchangers. Therefore, under most conditions, ionic interactions between the stationary phase and the charged sample components are part of the mechanism of separation. In our case, cationic styrenic and acrylic monoliths have also exhibited ubiquitous hydrophobic interactions leading to long retention times of peptides and proteins and peak broadening [16,18]. In order to suppress this effect, most commonly an organic solvent is added to the mobile phase.

The data in Fig. 12 were obtained by measuring both the electrosmotic flow and the streaming potential in columns packed with either octyl- or dodecylaminated styrenic monolithic stationary phases previously described. Phosphate buffer–acetonitrile mixture was employed as the mobile phase modulator. Particular attention was paid to the effect of the mobile phase composition on the $\zeta$-potential of the monolithic columns. As seen in Fig. 12, plots of $\zeta$-potential against percent ACN show that $\zeta$-potential has a minimum at 35% acetonitrile and then increases with the acetonitrile concentration up to 50%. Such behavior of $\zeta$-potential cannot be predicted simply from the solvent properties of the binary mixture, e.g. the dielectric constant to viscosity ratio [32].

The four chromatograms in Fig. 13 illustrate the effect of ACN concentration on the separation of two angiotensin-type peptides on the both columns. From the chromatograms it can be inferred that EOF

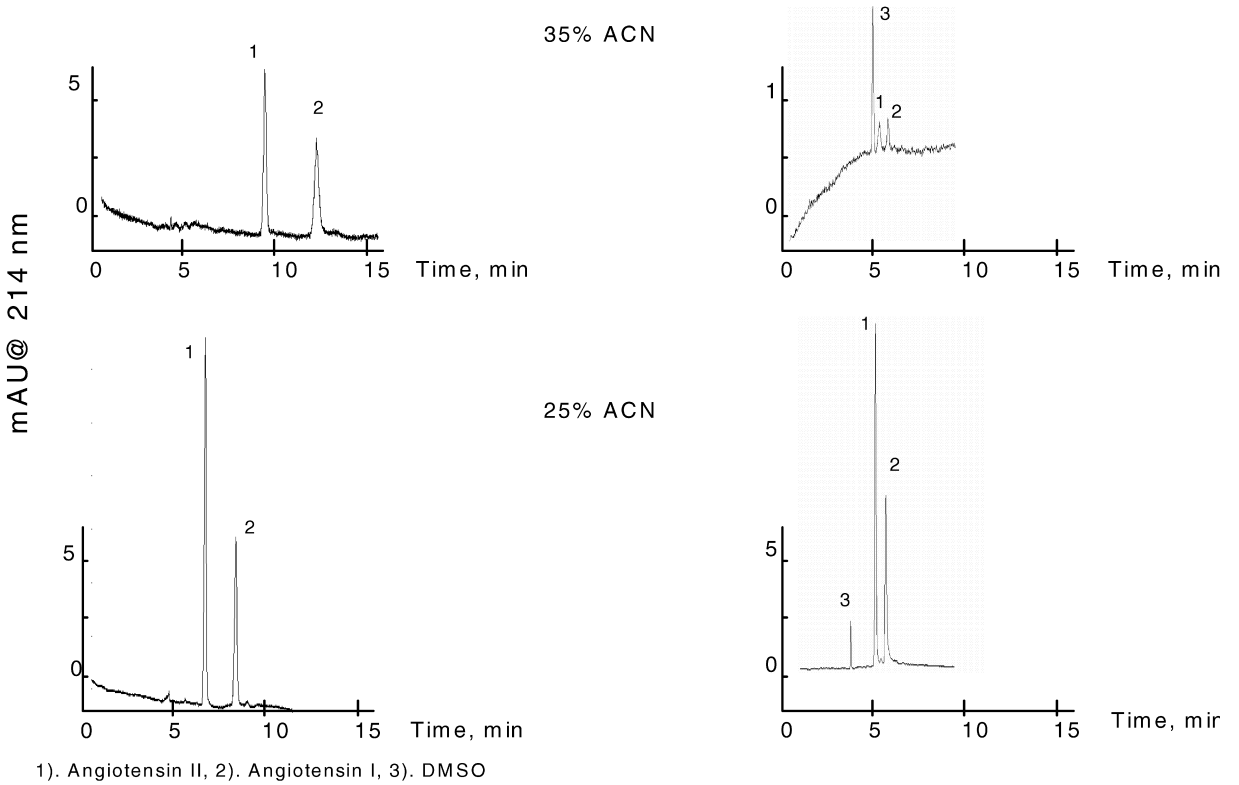


Fig. 13. Separation of the angiotensin-type peptides on octylated, Column VI, and dodecylated, Column VIII, porous monolithic polystyrene columns in 5 m*M* phosphate buffer, pH 3.0, 50 m*M* NaCl with various ACN concentrations.

velocity decreases at 35% ACN due to the decrease in $\zeta$-potential with concomitant decrease in the column efficiency and sample recovery probably due to increased electrostatic interactions. Thus, the basic peptides are less repelled from the less positively charged stationary phase at 35% of ACN in the running buffer. For Column VIII with dodecylaminated stationary phase, the effect of acetonitrile clearly manifests a drastic decrease in signal-to-noise ratio. These perturbations in the $\zeta$-potential could be imposed by the structure of the binary mixture. Mixtures of ACN and HOH exhibit anomalous thermodynamic properties, and this has led to the postulate of *microheterogeneity* [80], that means the solution can be separated into regions of ACN and regions of water.

Acetonitrile is a widely used solvent in liquid chromatography as it contains a hydrophobic methyl group connected to a hydrophilic cyano group and can thus be thought of as a small surfactant molecule. It is then not too surprising that agglomerization can lead to micromolecular structures as postulated by theories involving solvent microheterogeneity. Mixtures of ACN–water depending on macro-concentrations are capable of forming up to six different compositions on the microscopic scale [81]. It is reasonable to assume that changes in the microscopic structure of this solvent mixture with composition will affect the structure of the double-layer also. For instance, water structuring near the surface could control the location of the hydrodynamic shear plane, causing changes in $\zeta$-potential.

Furthermore, changes in the organization of the surface functional groups with addition of acetonitrile can be equivalent to a shift of the shear plane with concomitant changes in $\zeta$-potential according to the ''hairy'' surface model [82]. This assumes that the surface in contact with the electrolyte solution is covered with a molecular fur which may have a profound effect on the structure and thickness of the

double layer and concomitantly on the electrosmotic properties of the chromatographic column.

*4.3.2. Effect of alkyl chain length at the surface*

In order to assess the effect of the length of alkyl functions on the $\zeta$-potential a series of *n*-alkyl dimethyl amines of differing *n*-alkyl chain lengths ($N=2$, 4, 8, 12) were anchored to the surface of a monolithic porous support. The $\zeta$-potential was evaluated from data obtained by the measurements of both the EOF and the streaming potential as illustrated in Fig. 14. It is seen that in the carbon number range 2–12, the $\zeta$-potential first decreases and then increases with the length of the alkyl chains. The $\zeta$-potential has a minimum value at carbon number eight.

The results shown in Fig. 14 may be explained as follows. At low value of *N* the alkyl chains of the quaternary ammonium groups attached to the chromatographic surface are short, therefore the density of positive charges is high, but with increasing *N*, it decreases and a minimum is observed. After reaching a critical value of *N*, due to the effect of intercatenary interactions the density of accessible positive charges increases again. This interpretation is supported by the results by Sindorf et al. [64] who found by $^{13}$C NMR that the mobility of alkyl chains first increases with chain length up to $N=8$ but upon further increase in the chain length the chains acquire a semicrystalline form with concomitant increase in the accessible charge density. Additionally, IR spectroscopic and ellipsometric studies by Porter et al. [83] also show that the long *n*-alkyl thiols (about $N=18$) form a densely packed, ''crystalline'' assembly with fully extended alkyl chains. As the alkyl chain length decreases, the surface structure becomes increasingly disordered and thus ''liquid-like''. With our columns, this is accompanied by lower packing density and coverage as well as with the concomitant decrease in the surface charge density and $\zeta$-potential. The same minimum at $N=8$ was found in the studies of the $\zeta$-potential in quartz/*n*-alkane/water system by streaming potential measurements with a series of *n*-alkanes from hexane to pentadecane [84]. In view of these results we can infer from the data shown in Fig. 14, that both $C_4$ and $C_{12}$ columns are very similar in terms of electrosmotic behavior with similarly ''extended'' but less hydrophobic stationary phase on the butylaminated column. Thus, columns with the butylamine functionalities at the chromatographic surface could be the optimal stationary phase for separation of peptides and proteins. In fact, a very efficient isocratic separation of proteins by CEC was achieved recently with such columns [85] in our laboratory.

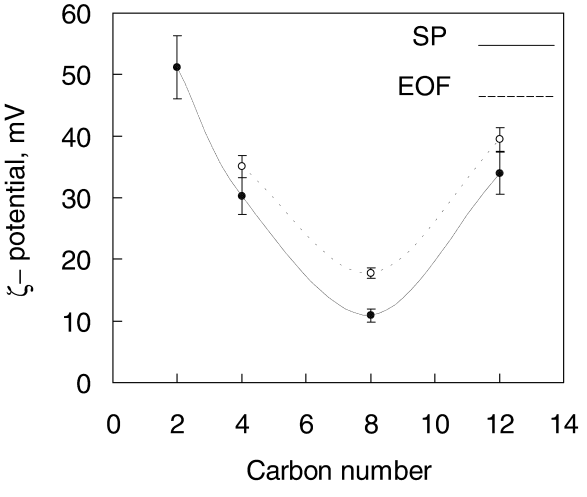


Fig. 14. Chain length effect on $\zeta$-potential evaluated from electrosmotic flow and streaming potential in 5 m*M* phosphate buffer, 25% ACN, 50 m*M* NaCl, pH 3.0; porous styrenic monolithic columns were functionalized with triethylamine, dimethylbutylamine, dimethyloctylamine and dimethyldodecylamine.

## 5. Conclusion

A high-pressure apparatus is presented for determining the $\zeta$-potential of porous monolithic packings formed in situ inside fused-silica capillaries by streaming potential measurements. This paper describes the set-up and some typical results obtained with it for capillary columns packed with a variety of stationary phases particularly interesting for CEC. Due to the high pressure employed in the experimental set-up, high velocities of the laminar flow and consequently, high values of electric potential drop could be achieved. This allowed the measurements in the region of high salt concentrations in the miniature packed capillary columns not applicable for

measurements by commercial instruments whose working pressure is limited to 0.4–0.5 bar.

Several modified, such as alkali-treated, polymer grafted with porous and nonporous layer fused-silica capillaries were characterized using streaming potential measurements. Also the $\zeta$-potential of different packings was evaluated in aqueous solutions under various physiochemical conditions. From pH dependence of the $\zeta$-potential, the potential determining ions are proved to be $H^+$ and $OH^-$ in polystyrene–water and fused-silica–water systems. The introduction of basic groups on to the styrene-based porous monolithic substrate by reductive amination manifests itself in the elimination of the isoelectric point and shift into the positive $\zeta$-potential range.

The potential applications of streaming potential measurements are demonstrated for optimization of chromatographic surfaces. Streaming potential measurements allow analyzing the interfacial charges of polymers of various shapes. Thus obtained information on surface charge can be correlated with retention behavior of the separated biopolymers, and can in this way be used for the optimization of surface modification procedures. Similarly, the quality control of packings employed can be based on streaming potential measurements.

Streaming potential measurements appear to provide information about the packings' $\zeta$-potential more simply and with less interference from other phenomena over a wide pH range, when compared with constant voltage electrosmosis under conditions of this study. The comparative study on determination of $\zeta_{EO}$ and $\zeta_{SP}$ is in reasonable agreement with earlier investigations on the similar fused-silica or oxide and polystyrenic systems. Data obtained with streaming potential measurements give better information on the behavior of the materials because temperature effects are hardly present. Using the streaming potential to calculate $\zeta$-potentials was found to be convenient and reliable, especially for the modified capillaries with very low $\zeta$-potential, which would result in low electrosmotic flows. Experimental results support the applicability of the streaming potential method as a means for determining the $\zeta$-potential of CEC packings.

The system constructed opens up the possibility for a complete characterization of the separation conditions, e.g. the capillary wall, influence of the duplex nature of the columns, stationary phase surface, and organic modifier concentration in the buffer, viscosity and temperature. Additionally, measurements of changes in streaming potential can be used to assess the results of a variety of surface modification strategies. Even without rigorous data analysis, electrokinetic measurements can provide insight to surface alteration, protein adsorption, longevity, and ionogenic features of different packings. A major advantage of the technique is the ability to investigate adsorption phenomena and the electrokinetic properties of surfaces in situ.

## Acknowledgements

This work was supported by Grant No. GM 20933 from the National Institute of Health, US Public Health Service. We are grateful to Victor Pantani of the Department of Physiology of the Yale School of Medicine, for the donation of the Keithley Electrometer and to Ilya Tyomkin for helpful discussions.

## References

[1] K.D. Bartle, R.A. Carney, A. Cavazza, M.G. Cikalo, P. Myers, M.M. Robson, S.C.P. Roulin, K. Sealey, J. Chromatogr. A 892 (2000) 279.
[2] R.J. Boughtflower, C.J. Paterson, J.H. Knox, J. Chromatogr. A 887 (2000) 409.
[3] G. Choudhary, Cs. Horváth, J. Chromatogr. A 781 (1997) 161.
[4] B.A. Grimes, J.J. Meyers, A.I. Liapis, J. Chromatogr. A 890 (2000) 61.
[5] C.G. Huber, G. Choudhary, Cs. Horváth, Anal. Chem. 69 (1997) 4429.
[6] S. Luedtke, T. Adam, N. von Doehren, K.K. Unger, J. Chromatogr. A 887 (2000) 339.
[7] N.W. Smith, A.S. Carter-Finch, J. Chromatogr. A 892 (2000) 219.
[8] E. Wen, R. Asiaie, Cs. Horváth, J. Chromatogr. A 855 (1999) 349.
[9] I. Gusev, X. Huang, Cs. Horváth, in: HPLC'97, 21st International Symposium on High performance Liquid Phase Separations and related techniques, Birmingham, UK, 1997, p. 170.
[10] E.C. Peters, M. Petro, F. Svec, J.M.J. Frechet, Anal. Chem. 69 (1997) 3646.
[11] R. Asiaie, X. Huang, D. Farnan, Cs. Horváth, J. Chromatogr. A 806 (1998) 251.

[12] B. He, F. Regnier, J. Pharm. Biomed. Anal. 17 (1998) 925.
[13] N. Tanaka, H. Nagayama, H. Kobayashi, T. Ikegami, K. Hosoya, N. Ishizuka, H. Minakuchi, K. Nakanishi, K. Cabrera, D. Lubda, HRC J. High Resolut. Chromatogr. 23 (2000) 111.
[14] G.S. Chirica, V.T. Remcho, Anal. Chem. 72 (2000) 3605.
[15] J. Zhang, X. Huang, S.H. Zhang, Cs. Horváth, Anal. Chem. 72 (2000) 3022.
[16] I. Gusev, X. Huang, Cs. Horváth, J. Chromatogr. A 855 (1999) 273.
[17] X. Huang, J. Zhang, Cs. Horváth, J. Chromatogr. A 858 (1999) 91.
[18] S.H. Zhang, X. Huang, J. Zhang, Cs. Horváth, J. Chromatogr. A 887 (2000) 465.
[19] K. Dorfner, in: K. Dorfner (Ed.), Ion Exchangers, Walter de Gruyter, Berlin, 1991, p. 241.
[20] R.J. Hunter, Zeta Potential in Colloid Science: Principles and Applications, Academic Press, London, 1981.
[21] F. Reuss, Mem. Soc. Naturalistes Moscou 2 (1809) 327.
[22] G. Quincke, Pogg. Ann. 113 (1861) 513.
[23] M. von Smoluchowski, Electric Endosmosis and Streaming Current, Ann Arbor Press, Ann Arbor, MI, 1951.
[24] R.J. Hunter, Coll. Sci. 16 (1961) 190.
[25] S.S. Dukhin, B.V. Derjaguin, in: E. Matijevic (Editor), Surface and Colloid Science, Wiley, New York, 1974, p. 148.
[26] J.T.G. Overbeek, in: H.R. Kruyt (Ed.), Colloid Science, Elsevier, Amsterdam, 1952, Chapter 5.
[27] A.J. Ham, H.W. Douglas, Trans. Faraday Soc. 44 (1948) 955.
[28] G.J. Biefer, S.G. Mason, Coll. Sci. 9 (1954) 20.
[29] A. Kitahara, S. Katano, T. Fujii, Bull. Chem. Soc. Jpn. 44 (1971) 3242.
[30] M. Rasmusson, S. Wall, J. Colloid. Interf. Sci. 209 (1999) 312.
[31] C.L. Rice, R.J. Whitehead, Phys. Chem. 69 (1965) 4017.
[32] C. Schwer, E. Kenndler, Anal. Chem. 63 (1991) 1801.
[33] M. von Smoluchowski, Bull. Int. Acad. Sci. Cracovie 1 (1903) 184.
[34] J.C. Reijenga, G.V.A. Aben, T. Verheggen, F.M. Everaerts, J. Chromatogr. 260 (1983) 241.
[35] Z.M. Zorin, V.I. Lashnev, M.P. Sidorova, V.D. Sobolev, N.V. Churaev, Coll. J. USSR 39 (1977) 1012.
[36] J.S. Lyons, D.N. Furlong, A. Homola, T.W. Healy, Aust. J. Chem. 34 (1981) 1167.
[37] D. Fairhurst, V. Ribitsch, ACS Symp. Ser. 472 (1991) 337.
[38] P.J. Scales, F. Grieser, T.W. Healy, L.R. White, D.Y.C. Chan, Langmuir 8 (1992) 965.
[39] S.E. Truesdail, G.B. Westermann-Clark, D.O. Shah, J. Environ. Eng. ASCE 124 (1998) 1228.
[40] M. Elimelech, W.H. Chen, J.J. Waypa, Desalination 95 (1994) 269.
[41] R.C. Weast, M.J. Astle, W.H. Beyer (Eds.), CRC Handbook of Chemistry and Physics, CRC Press, Boca Raton, FL, 1984, p. F9.
[42] X. Huang, Cs. Horváth, J. Chromatogr. A 788 (1997) 155.
[43] A. Bismarck, M.E. Kumru, J. Springer, J. Colloid. Interf. Sci. 217 (1999) 377.
[44] W. Carius, B. Dobias, Coll. Polym. Sci. 259 (1981) 470.
[45] A.E. Childress, M. Elimelech, Environ. Sci. Technol. 34 (2000) 3710.
[46] N.V. Churaev, I.P. Sergeeva, V.D. Sobolev, D.E. Ulberg, J. Colloid. Interf. Sci. 151 (1992) 490.
[47] H.J. Jacobasch, F. Simon, C. Werner, C. Bellmann, Tech. Mes. 63 (1996) 447.
[48] M.C. Wilbert, S. Delagah, J. Pellegrino, J. Membr. Sci. 161 (1999) 247.
[49] D.B. Pengra, P.-Z. Wong, in: Mater. Res. Soc. Symp. Proc., Materials Research Society, 1997.
[50] R.A. Van Wagenen, J.D. Andrade, J.B. Hibbs, J. Electrochem. Soc. 123 (1976) 1438.
[51] R.E. Majors, in: Cs. Horváth (Ed.), High-Performance Liquid Chromatography, Academic Press, New York, 1980, p. 82.
[52] R.A. Van Wagenen, J.D. Andrade, J. Colloid. Interf. Sci. 76 (1980) 305.
[53] A.J. Rutgers, M. Desmet, G. Demyer, Trans. Faraday Soc. 53 (1957) 393.
[54] P.R. Stewart, N. Street, Coll. Sci. 16 (1961) 192.
[55] A.J. Vanderlinde, B.H. Bijsterbosch, Colloids Surfaces 41 (1989) 345.
[56] R. Stol, W.T. Kok, H. Poppe, in: HPCE'01, Boston, MA, USA, 2001.
[57] S. Schwarz, K. Lunkwitz, B. Kessler, U. Spiegler, E. Killmann, W. Jaeger, Colloids Surfaces A Phys. Eng. Asp. 163 (2000) 17.
[58] C. Werner, U. Konig, A. Augsburg, C. Arnhold, H. Korber, R. Zimmermann, H.J. Jacobasch, Colloids Surfaces A Phys. Eng. Asp. 159 (1999) 519.
[59] J.Y. Chen, C.-H. Ko, S. Bhattacharjee, M. Elimelech, Colloids Surfaces A Phys. Eng. Asp. 191 (2001) 3.
[60] P.R. Johnson, J. Colloid. Interf. Sci. 209 (1999) 264.
[61] P.C. Hiemenz, R. Rajagopalan, Principles of Colloid and Surface Chemistry, Marcel Dekker, New York, 1997.
[62] F.M. Fowkes, F.H. Hielscher, Abstr. Papers Am. Chem. Soc. 179 (1980) 29.
[63] J. Lyklema, Fundamentals of Interface and Colloid Science, Academic Press, London, 1995.
[64] D.W. Sindorf, G.E. Maciel, J. Am. Chem. Soc. 105 (1983) 1848.
[65] N.G. Korzhenevskaya, M.M. Mestechkin, S.N. Lyashchuk, Z. Org. Khim. 32 (1996) 498.
[66] W. Schutzner, E. Kenndler, Anal. Chem. 64 (1992) 1991.
[67] C.C. Christoforou, G.B. Westermannclark, J.L. Anderson, J. Colloid. Interf. Sci. 106 (1985) 1.
[68] O. El-Gholabzouri, M.A. Cabrerizo, R. Hidalgo-Alvarez, Colloids Surfaces A Phys. Eng. Asp. 159 (1999) 449.
[69] P. Fievet, A. Szymczyk, B. Aoubiza, J. Pagetti, J. Membr. Sci. 168 (2000) 87.
[70] R. Hidalgoalvarez, Adv. Colloid Sci. 34 (1991) 217.
[71] R. Hidalgoalvarez, F.J.D. Nieves, G. Pardo, J. Colloid. Interf. Sci. 107 (1985) 295.
[72] I.H. Huisman, P. Pradanos, J.I. Calvo, A. Hernandez, J. Membr. Sci. 178 (2000) 79.
[73] K.J. Kim, A.G. Fane, M. Nystrom, A. Pihlajamaki, W.R. Bowen, H. Mukhtar, J. Membr. Sci. 116 (1996) 149.
[74] A. Szymczyk, P. Fievet, M. Mullet, J.C. Reggiani, J. Pagetti, Desalination 119 (1998) 309.

[75] J. Lyklema, in: J.D. Andrade (Ed.), Surface and Interfacial Aspects of Biomedical Polymers, Plenum Press, New York, 1985, p. 293.
[76] S. Terabe, K. Otsuka, T. Ando, Anal. Chem. 57 (1985) 834.
[77] P. Grossman, in: P.D. Grossman, J.C. Colburn (Eds.), Capillary Electrophoresis, Academic Press, San Diego, CA, 1992, p. 3.
[78] A. Szymczyk, A. Pierre, J.C. Reggiani, J. Pagetti, J. Membr. Sci. 134 (1997) 59.
[79] C.J. Vanoss, M.K. Chaudhury, R.J. Good, Chem. Rev. 88 (1988) 927.
[80] H. Kovacs, A. Laaksonen, J. Am. Chem. Soc. 113 (1991) 5596.
[81] K.L. Rowlen, J.M. Harris, Anal. Chem. 63 (1991) 964.
[82] R. Folkersma, A.J.G. van Diemen, H.N. Stein, Langmuir 14 (1998) 5973.
[83] M.D. Porter, T.B. Bright, D.L. Allara, C.E.D. Chidsey, J. Am. Chem. Soc. 109 (1987) 3559.
[84] B. Janczuk, E. Chibowski, Mater. Chem. Phys. 12 (1985) 367.
[85] S.H. Zhang, J. Zhang, Cs. Horváth, J. Chromatogr. A 914 (2001) 189.